Journal of Power Sources 194 (2009) 967–971

Contents lists available at ScienceDirect

Journal of Power Sources

journal homepage: www.elsevier.com/locate/jpowsour

Short communication

A high performance intermediate temperature fuel cell based on a thick oxide–carbonate electrolyte

Lei Zhang[a], Rong Lan[a], Xiaoxiang Xu[b], Shanwen Tao[a,b,*], Yinzhu Jiang[a], Arno Kraft[a]

[a] Department of Chemistry, Heriot-Watt University, Edinburgh EH14 4AS, UK
[b] School of Chemistry, University of St. Andrews, St Andrews, Fife KY16 9ST, UK

ARTICLE INFO

Article history:
Received 24 April 2009
Received in revised form 12 June 2009
Accepted 17 June 2009
Available online 25 June 2009

Keywords:
Intermediate temperature
Fuel cell
Co-doped ceria
Composite electrolyte

ABSTRACT

A high performance intermediate temperature fuel cell (ITFC) with composite electrolyte composed of co-doped ceria $Ce_{0.8}Gd_{0.05}Y_{0.15}O_{1.9}$ (GYDC) and a binary carbonate-based (52 mol% Li_2CO_3/48 mol% Na_2CO_3), 1.2 mm thick electrolyte layer has been developed. Co-doped $Ce_{0.8}Gd_{0.05}Y_{0.15}O_{1.9}$ was synthesized by a glycine–nitrate process and used as solid support matrix for the composite electrolyte. The conductivity of both composite electrolyte and GYDC supporting substrate were measured by AC impedance spectroscopy. It showed a sharp conductivity jump at about 500 °C when the carbonates melted. Single cells with thick electrolyte layer were fabricated by a dry-pressing technique using NiO as anode and $Ba_{0.5}Sr_{0.5}Co_{0.8}Fe_{0.2}O_{3-\delta}$ or lithiated NiO as cathode. The cell was tested at 450–550 °C using hydrogen as the fuel and air as the oxidant. Excellent performance with high power density of 670 mW cm^{-2} at 550 °C was achieved for a 1.2 mm thick composite electrolyte containing 40 wt% carbonates which is much higher than that of a cell based on pure GYDC with a 70 μm thick electrolyte layer.

1. Introduction

Fuel cells are important electrochemical devices which can directly convert chemical energy into electricity at high efficiency [1–5]. Fuel cells have a wide range of applications in stationary power generation, transport and portable devices. High temperature solid oxide fuel cells (SOFCs) have been studied extensively in the past decades. Conventional SOFCs with yttrium-stabilized zirconia (YSZ) electrolyte need a high operating temperature (700–900 °C) to achieve the required conductivity. The durability of conventional SOFCs is still not yet good enough due to materials and microstructure degradation at high temperature. Therefore, intermediate temperature fuel cells (ITFCs) working between 150 and 600 °C have attracted the attention of many researchers [6–8]. The key challenge of ITFCs is to develop a good electrolyte material with sufficient ionic conductivity in the intermediate temperature range. Doped ceria was an exciting discovery due to its high ionic conductivity at relatively low temperatures although the electronic conduction becomes significant at a temperature above 550 °C [9–15]. Recently, it has been reported that Gd^{3+} and Y^{3+} co-doped ceria exhibits enhanced conductivity at 400–700 °C compared to sole-doped ceria [16]. The co-doped ceria with composition $Ce_{0.8}Gd_{0.05}Y_{0.15}O_{1.9}$ showed particularly high ionic conductivity of 0.01 S cm^{-1} at 500 °C according to their study, which makes it a promising electrolyte material for intermediate temperature fuel cells. Also, a series of novel materials called solid carbonate-ceria composite (SCC) electrolytes were reported by Zhu et al. [17,18]. According to their research, these new SCC materials have demonstrated high ionic conductivity (10^{-2} to 1.0 S cm^{-1}) in the intermediate temperature region. Huang et al. [19] developed intermediate temperature fuel cells with a ceria-based composite electrolyte $Ce_{0.8}Sm_{0.2}O_{1.9}$ (SDC) containing 30 wt% ($2Li_2CO_3$:$1Na_2CO_3$). They observed higher open circuit voltage (OCV) in a cell with an electrolyte thickness of 0.5 mm compared to one where the thickness was only 0.3 mm. This was attributed to the porous microstructure of the electrolyte. However, in our experiments, it was found that the OCV is also lower when a thin SCC electrolyte layer was used even though the electrolyte was reasonable dense. Cells with thicker electrolyte layer exhibited a higher OCV and better performance.

In a fuel cell, in order to achieve low ohmic resistance, the thickness of electrolyte is normally kept as thin as possible as long it is gas-tight and the mechanical properties are not affected. Normally a thickness of 10–100 μm is preferred for solid oxide fuel cells. As for molten carbonate fuel cells (MCFCs), the thickness of carbonate–$LiAlO_2$ composite electrolyte is normally 500–600 μm [20]. In this work, we used newly developed low temperature high conductivity co-doped ceria $Ce_{0.8}Gd_{0.05}Y_{0.15}O_{1.9}$ as support substrate for a carbonate-ceria composite electrolyte. The conductivity was measured and compared between single-doped, co-doped and

* Corresponding author at: Chemistry, School of Engineering & Physical Sciences, Heriot-Watt University, Edinburgh EH14 4AS, UK. Tel.: +44 0 131 451 4299; fax: +44 0 131 451 3180.
E-mail address: s.tao@hw.ac.uk (S. Tao).

0378-7753/$ – see front matter © 2009 Elsevier B.V. All rights reserved.
doi:10.1016/j.jpowsour.2009.06.062

composite materials as electrolytes. Single cells with pure oxide and oxide–carbonate composite electrolytes were fabricated and demonstrated good performance in a H_2/air cell with a 1.2 mm thick SCC electrolyte.

2. Experimental

2.1. Synthesis of $Ce_{0.8}Gd_{0.05}Y_{0.15}O_{1.9}$ powders by a combustion method

Gd^{3+} and Y^{3+} co-doped CeO_2 with composition of $Ce_{0.8}Gd_{0.05}Y_{0.15}O_{1.9}$ (GYDC) was synthesized by the combustion technique using glycine–nitrate method [20]. Stoichiometric amounts of cerium nitride hexahydrate $Ce(NO_3)_3{\cdot}6H_2O$ and yttrium nitrate hexahydrate $Y(NO_3)_3{\cdot}6H_2O$ were mixed and dissolved in deionized water. Gadolinium oxide Gd_2O_3 was dissolved in nitric acid to form gadolinium nitrate. The solution was heated on a hot plate to 70 °C. A homogeneous solution was obtained with continually stirring. Glycine (NH_2CH_2COOH) was then added until a glycine/nitrate molar ratio of 0.5 was reached. The nitrate solution was concentrated gradually in an alumina crucible until all the residual water had evaporated. Finally, spontaneous ignition occurred and the combustion reaction completed within a few seconds, leaving a pale yellow and porous ash in the container. A fine-mesh metal box was used to cover the container to prevent the ash from flying outside during the combustion step. The as-collected ash was further heated at 600 °C for 2 h in air to obtain pure, single phase co-doped ceria powders. A schematic program for preparation of CGYO powders is shown in Fig. 1.

2.2. Preparation of $Ce_{0.8}Gd_{0.05}Y_{0.15}O_{1.9}$ pellets for conductivity measurements

For conductivity measurements, powders were uniaxially dry-pressed into pellets at 38 MPa and sintered at 1350 °C for 5 h in a tube furnace. For comparison, single-doped ceria $Ce_{0.8}Gd_{0.2}O_{1.9}$ was also synthesized using the same process. $Ba_{0.5}Sr_{0.5}Co_{0.8}Fe_{0.2}O_{3-\delta}$ (BSCF) cathode material was made by the same method with appropriate stoichiometric precursors of $Ba(NO_3)_3$, $Sr(NO_3)_2$, $Co(NO_3)_2{\cdot}6H_2O$ and $Fe(NO_3)_3{\cdot}9H_2O$. The dark black powders were collected and calcined at 1000 °C for 4 h to get a single phase.

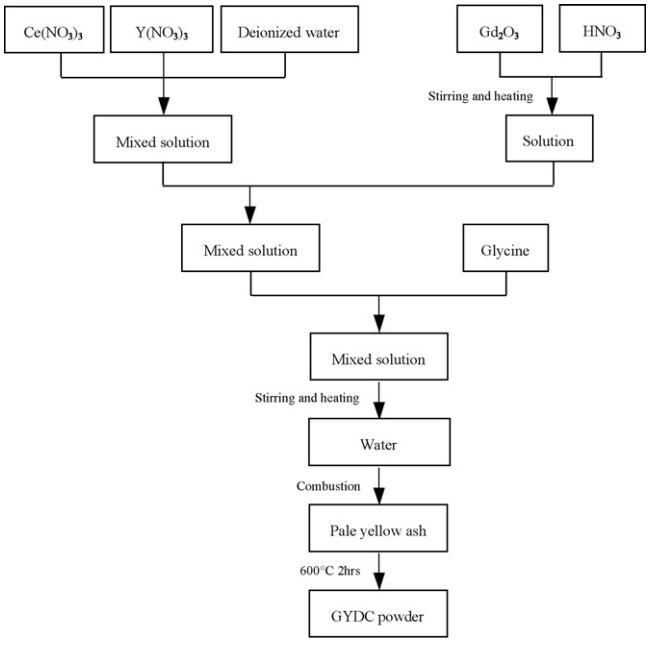

Fig. 1. The schematic program for the preparation of GYDC powder.

2.3. Fabrication of fuel cell based on $Ce_{0.8}Gd_{0.05}Y_{0.15}O_{1.9}$ electrolyte

Single cells were fabricated by dry-pressing. Commercial NiO (65 wt%) and CGYO (35 wt%) powders were mixed and ground with alcohol for 2 h. After the alcohol had been evaporated, the dried mixture was first pressed under 38 MPa onto a substrate in a stainless steel die. CGYO powder was added and co-pressed at 38 MPa to form a green bilayer that was subsequently co-fired at 1350 °C in air for 5 h which densified the CGYO film. The final thickness of the CGYO layer was about 70 μm. The total thickness of the electrolyte–anode substrate assembly was about 1 mm. To prepare the composite cathode, BSCF powder (50 wt%) and CGYO powder (50 wt%) were mixed with an organic binder to form an ink. The electrolyte side of the electrolyte–anode bilayer was painted in the centre with this ink which gave a cathode area of 1.26 cm^2. The electrode was then sintered at 1050 °C for 2 h. To minimize the contact resistance, Silver paste was painted on both anode and cathode surface to serve as a current-collector.

2.4. Fabrication of fuel cell based on $Ce_{0.8}Gd_{0.05}Y_{0.15}O_{1.9}$/carbonate composite electrolyte

The $Ce_{0.8}Gd_{0.05}Y_{0.15}O_{1.9}$/carbonate composite material was made as follows. A mixture of lithium carbonate and sodium carbonate salts $(Li/Na)_2CO_3$ was prepared by combining Li_2CO_3 and Na_2CO_3 at a molar ratio of 52/48. GYDC powder (60 wt%) and $(Li/Na)_2CO_3$ (40 wt%) were mixed and ground thoroughly. The mixture was heated in air at 680 °C for 40 min and then taken out directly to air for cooling. The powder was ground again to provide the composite electrolyte.

The single cell was fabricated using a simple one-step dry-pressing process. The composite anode consisted of a mixture of NiO (50 wt%) and electrolyte (50 wt%). The composite cathode powder was composed of lithiated NiO (50 wt%) mixed with electrolyte (50 wt%). The anode, electrolyte and cathode were pressed into a pellet at a pressure of 300 MPa and then sintered at 600 °C for 1 h in air. The effective working area of the pellet was 1.26 cm^2. Silver paste was coated afterwards on each electrode surface to improve the electrical contact.

2.5. Materials characterization and fuel cell measurements

X-ray diffraction was performed using a Bruker-AXS D8 diffractometer (40 kV, 30 mA), controlled by DIFFRACT^{plus} software, in the Bragg–Brentano reflection geometry with Cu Kα radiation (λ = 1.5418 Å). The microstructures of the cell cross were inspected by using scanning electron microscopy (SEM) on a JEOL 5600 SEM operated at 20 kV.

AC impedance spectroscopy and cell tests were carried out using a Schlumberger Solartron 1250 Frequency Response Analyser which was coupled to a 1287 Electrochemical Interface and controlled by Z-plot electrochemical impedance software. The impedance spectra were recorded with a 100 mV AC signal amplitude over the frequency range 10^5~0.01 Hz. Fuel cell tests were carried out on a Solartron 1287 electrochemical interface using software CorrWare/CorrView for automatic data collection. Wet hydrogen (~3%H_2O by volume) with a flow rate 100 ml min^{-1} was supplied to the cell by passing the gas through room temperature water. The cathode side was open to air.

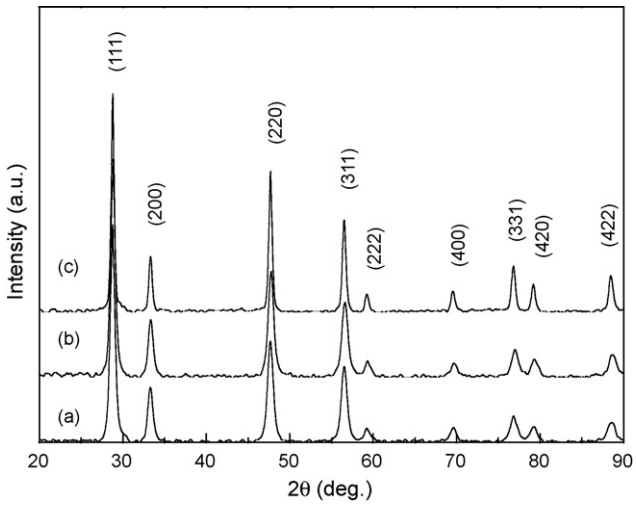

Fig. 2. X-ray diffraction patterns of (a) $Ce_{0.8}Gd_{0.2}O_{1.9}$, (b) $Ce_{0.8}Gd_{0.05}Y_{0.15}O_{1.9}$ and (c) composite electrolyte.

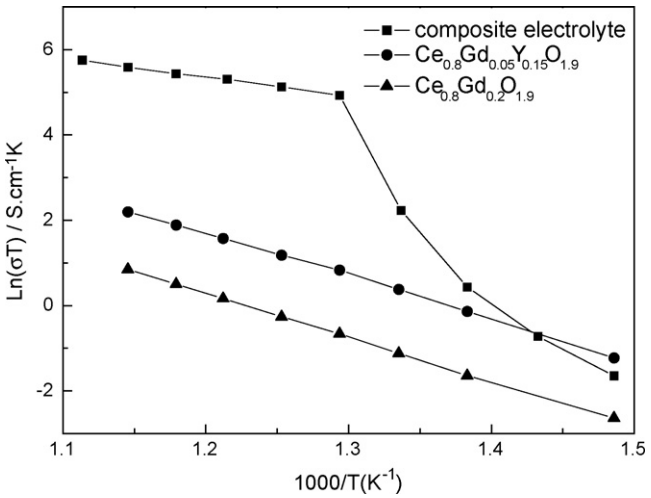

Fig. 3. Arrhenius plots for conductivity measurements of composite electrolyte compared to $Ce_{0.8}Gd_{0.2}O_{1.9}$ and $Ce_{0.8}Gd_{0.05}Y_{0.15}O_{1.9}$.

3. Results and discussion

3.1. XRD analysis

Fig. 2 shows the X-ray diffraction patterns of single-doped ceria $Ce_{0.8}Gd_{0.2}O_{1.9}$, co-doped ceria $Ce_{0.8}Gd_{0.05}Y_{0.15}O_{1.9}$ and a composite electrolyte (60 wt% CGYO + 40 wt% $(Li/Na)_2CO_3$). All powders exhibit single phase cubic structure. As mentioned above, the composite electrolyte was processed by heat treatment at 680 °C for 40 min and quenched in air thereafter. It can be seen that only one distinct phase of CGYO pattern is observed in the composite due to the carbonates being amorphous following the heat treatment. This has been proven by other researchers [21]. Lattice parameters for all samples were calculated by TOPAS software and gave $a = 5.4253(5)$ Å for $Ce_{0.8}Gd_{0.2}O_{1.9}$ and $a = 5.4135(1)$ Å for $Ce_{0.8}Gd_{0.05}Y_{0.15}O_{1.9}$. At a co-ordination number of eight, the ionic radius of Gd^{3+} (1.06 Å) is larger than that of Y^{3+} (1.015 Å) [22]. Lattice contraction was observed when large Gd^{3+} ions were replaced by smaller Y^{3+} ions. In $Ce_{0.8}Gd_{0.05}Y_{0.15}O_{1.9}$–carbonate, the lattice parameter for $Ce_{0.8}Gd_{0.05}Y_{0.15}O_{1.9}$ is $a = 5.4128(5)$ Å which is close within standard error to that of pure $Ce_{0.8}Gd_{0.05}Y_{0.15}O_{1.9}$. The solubility of Li^+ or Na^+ ions in $Ce_{0.8}Gd_{0.05}Y_{0.15}O_{1.9}$ lattice is very limited. No peaks of Li_2CO_3 or Na_2CO_3 were observed indicating that the carbonates are in an amorphous state in the composite.

3.2. Conductivity of the oxide and oxide–carbonate composite

Conductivity measurements were made in the temperature range of 400–600 °C. As shown in Fig. 3, co-doped GYDC shows apparently higher conductivity than solely doped GDC in the whole temperature range which agrees with the work of Guan et al. [16] and reconfirms the high conductivity of co-doped GYDC at intermediate temperature. The bulk and grain boundary responses cannot be separated and therefore only total conductivity was measured. It should be noted that the conductivity values obtained here are lower than those reported in the literature, which could be attributed to a different precursor source. It has been reported that the presence of a small amount of impurity such as SiO_2 can significantly increase the resistance at grain boundaries [23]. The conductivity of the composite electrolyte is much higher than that of both single and double doped ceria (Fig. 3). A sharp conductivity jump started at 475 °C (0.01 S cm^{-1}) and reached 0.18 S cm^{-1} at 500 °C which happens to be the melting point of binary $(Li/Na)_2CO_3$ [24]. This finding is different from the work of Huang et al. [19] who reported a conductivity jump at 475 °C which is 25 °C lower than the melting point. Zhu et al. [25] observed similar results by studying composite materials based on samarium doped ceria (SDC) and $(Li/K)_2CO_3$ carbonates. Superionic conductors are solid state materials with exceptionally high ionic conductivity by allowing the macroscopic movement of ions [26]. Huang et al. supposed that the formation of space charge zones in the interfacial regions leads

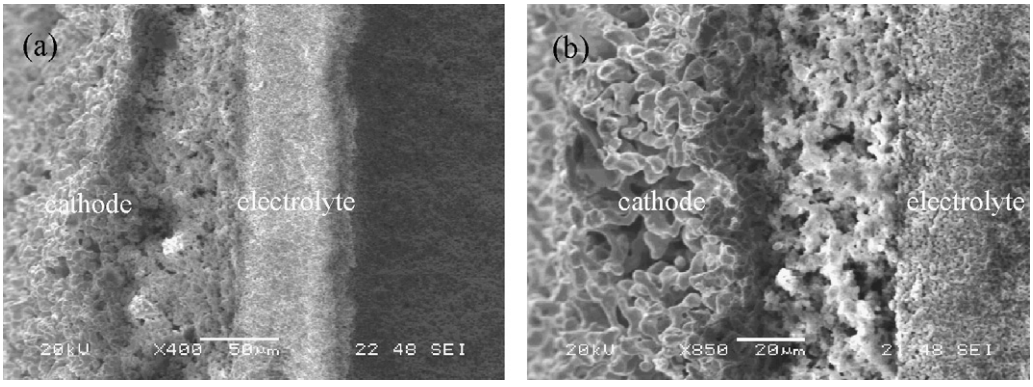

Fig. 4. Cross-sectional scanning electron micrographs of anode-supported cell: (a) entire cell at low magnification (left layer: cathode; middle layer: electrolyte; right layer: anode support); (b) BSCF cathode.

to the defects concentrations much higher than in the bulk. When the temperature exceeds 500 °C, the carbonates start to melt which greatly enhances the mobility of various ions (Na^+, Li^+, H^+, CO_3^{2-} and O^{2-}), leading to superionic conduction. The measured high conductivity in air above the melting point of carbonates should include all mobile ions. At high temperature, all ions become more mobile in the molten carbonates. In this case, although oxygen ions also contribute to the total conductivity in the GYDC phase, CO_3^{2-} ions could become the dominant contributor to the overall conductivity of the material [26]. In contrast, the ions are not activated and much less mobile below the melting temperature of the carbonates.

3.3. Fuel cell performance based on pure $Ce_{0.8}Gd_{0.05}Y_{0.15}O_{1.9}$ electrolyte

Single cells with pure CGYO electrolyte and BSCF cathode were fabricated by dry-pressing. In order to minimize the electrolyte resistance during low-temperature operation, great efforts were made to try different fabrication methods. After fuel cell testing, the microstructure of the cross-sectional area between a CGYO electrolyte, a BSCF cathode and a Ni-CGYO cermet anode was investigated by SEM. Fig. 4 shows the SEM morphology pictures of the cross-sectional area. It shows that the CGYO electrolyte layer is about 70 μm thick and is sandwiched between a porous cathode (left layer) and a porous anode (right layer) (see Fig. 4b). The cathode/electrolyte interface is not ideal due to the difference in thermal expansion co-efficients. Good anode/electrolyte interfaces was achieved. Additional refining and optimizing the microstructure of the electrodes, especially the porosity of anode, may further enhance the cell performance.

The single cell performance was tested using hydrogen as fuel and air as oxidant in the temperature range between 450 and 550 °C. The voltages and the corresponding power densities are shown in Fig. 5 as a function of current density. An open-circuit voltage (OCV) of 0.93 V is achieved at 475 °C. However, this value still

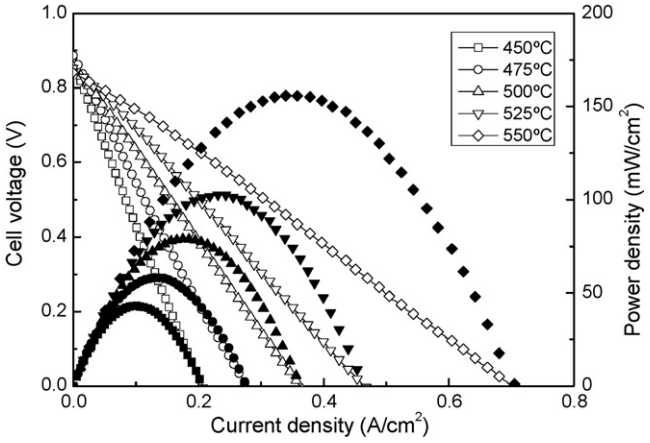

Fig. 5. Cell voltages (open symbols) and power densities (solid symbols) as function of current density of anode-supported cell, consisting of 50 μm CGYO electrolyte, BSCF cathode and Ni-CGYO anode; measured in hydrogen and air in temperature range of 450–550 °C.

displays a large deviation from the theoretical voltage and keeps decreasing to 0.88 V when the temperature is raised to 550 °C. The phenomenon should result from the electronic conductivity of doped-ceria materials induced by the reduction of Ce^{4+} to Ce^{3+} in reducing atmospheres [27,28]. The maximum power densities were 43, 79 and 155 mW cm^{-2} at 450, 500 and 550 °C, respectively. Further improvements can be made to enhance the cell performance by decreasing the electrolyte thickness and improving the cathode/electrolyte interface.

3.4. Fuel cell performance based on oxide–carbonate electrolyte

The SEM pictures of the single cell (before test) with GYDC–carbonate composite electrolyte shows the successful formation

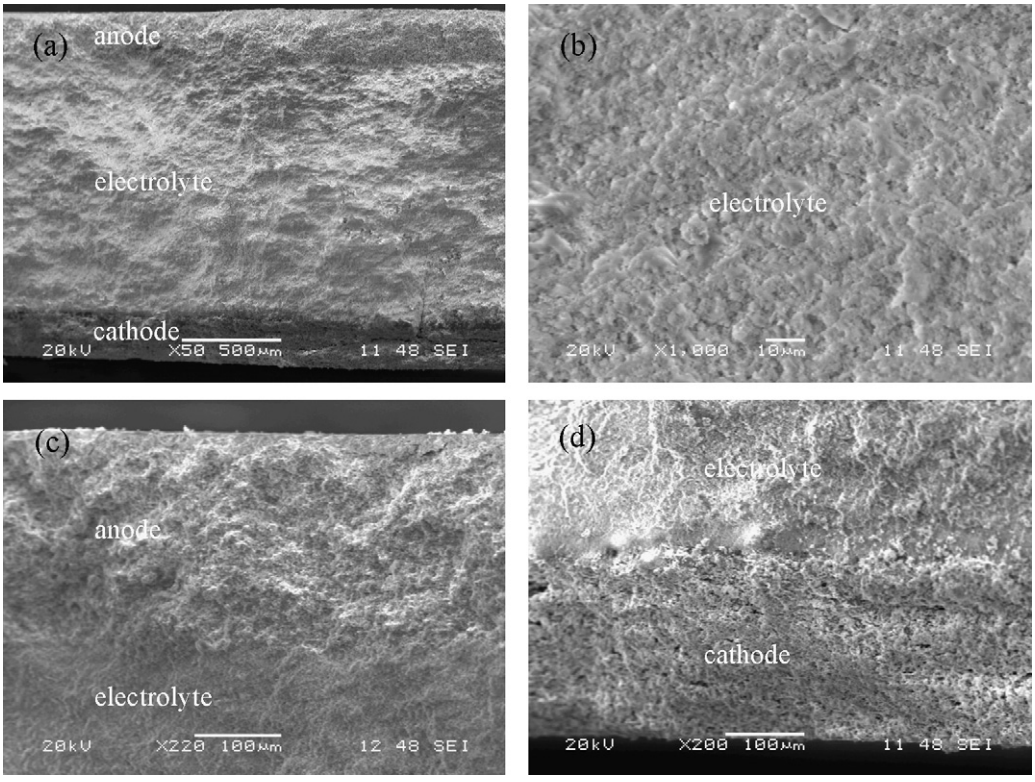

Fig. 6. Cross-sectional scanning electron micrographs of anode-supported cell: (a) entire cell at low magnification (upper layer: anode; middle layer: electrolyte; lower layer: cathode); (b) electrolyte; (c) electrolyte with anode; (d) electrolyte with cathode.

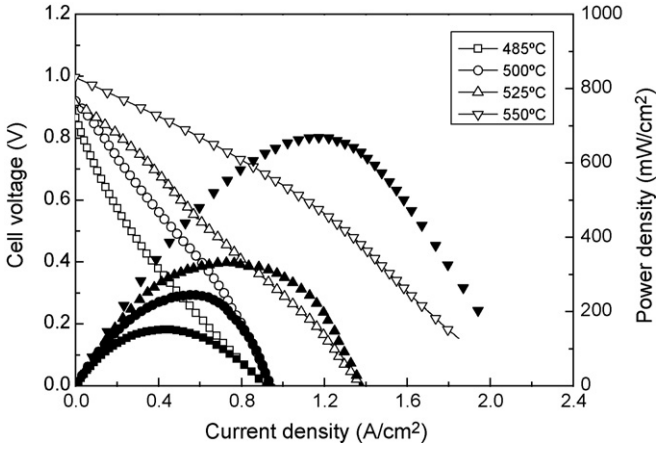

Fig. 7. Cell voltages (open symbols) and power densities (solid symbols) as function of current density of ITFC with composite electrolyte measured in hydrogen and air in the temperature range of 485–550 °C.

of a homogenous composite electrolyte with a porous cathode (Fig. 6). They also confirm a good contact between electrolyte and electrodes due to the simple one-step dry-pressing technique. Although the composite electrolyte can be pressed into a relatively dense layer during its fabrication, it cannot reach full density due to the low sintering temperature (600 °C). GYDC can be regarded as matrix in the composite electrolyte and, when the temperature reaches the melting point of the carbonates, the molten carbonates will fill the interspaces in the GYDC substrate to form a relatively dense composite electrolyte. Therefore, a good and homogenous substrate (GYDC in this case) will result in a much denser electrolyte layer. In contrast, the carbonates phase will begin to coagulate when the temperature decreases below its melting point when the change in microstructure of the electrolyte leads to the presence of a less dense electrolyte with small closed pores, as shown in Fig. 6b.

The single cell performance was tested using hydrogen as fuel and air as oxidant in the temperature range 485–550 °C. The voltages and the corresponding power densities as a function of current density are shown in Fig. 7. Open-circuit voltages (OCV) of 0.91, 0.95, 0.96 and 1.04 V are achieved at 485, 500, 525 and 550 °C, respectively. These values are higher than those of typical GDC fuel cells indicating that the addition of carbonates greatly suppresses the reduction of Ce^{4+} to Ce^{3+} [29,30]. Also, the OCV values increase with increasing operation temperature because more carbonates melt to fill in the pores inside the electrolyte helping to avoid any gas crossover. This indicates that the electrolyte is gas-tight. Excellent performances were obtained with a maximum power density of 670 mW cm^{-2} at 550 °C for a H_2/air fuel cell with a 1.2 mm thick electrolyte. Such excellent performances can be attributed to superionic conduction of the composite electrolyte above the melting point of the carbonate. The doped ceria–carbonate composite ionic conductor can be considered as a kind of molten carbonate electrolyte. Besides CO_3^{2-}, O^{2-} ions also contribute to conduction as doped ceria is a well-known oxygen ion conductor. It should be noted that doped ceria can be a proton-conductor as well in a reducing atmosphere [31,32]. Proton conduction is also possible through the transfer of *in situ* formed HCO_3^{2-} ions in the presence of H_2.

4. Conclusions

It has been observed that co-doping of Gd^{3+} and Y^{3+} ions can increase the total conductivity of Gd-doped ceria. High conductivity was observed in oxide–carbonate composites based on co-doped ceria ($Ce_{0.8}Gd_{0.05}Y_{0.15}O_{1.9}$ GYDC) and binary $(Li/Na)_2CO_3$ salt. It is believed that the melting of carbonates greatly enhanced the mobility of ions in materials leading to superionic conduction, which is the key factor for the high performance of this composite. The composite can be regarded as a combination of ceramic O^{2-} ion conductor and molten carbonate salts.

Single cells were fabricated using a one-step dry-pressing technique. Excellent cell performances with high power densities up to 670 mW cm^{-2} at 550 °C were achieved indicating a good composite electrolyte material for further ITFC development. At 550 °C, the fuel cell performance with a 1.2 mm thick composite electrolyte was much higher than one with only a 70 μm thick pure $Ce_{0.8}Gd_{0.05}Y_{0.15}O_{1.9}$ electrolyte layer although the cell with pure oxide electrolyte is not well optimized. The ionic conductivity of the composite is so high that the use of a thick electrolyte will not lead to big ohmic resistance loss. On the contrary, low OCV and poor performance were observed when a thin electrolyte was used.

Acknowledgements

We thank EPSRC for funding. One of the authors (Xu) thanks EastCHEM for a studentship. We are grateful to Prof. John T.S. Irvine at University of St Andrews for kind support.

References

[1] B.C.H. Steele, A. Heinzel, Nature 414 (2001) 345–352.
[2] S.P. Jiang, S.H. Chan, J. Mater. Sci. 39 (2004) 4405–4439.
[3] S.W. Tao, J.T.S. Irvine, Nat. Mater. 2 (2003) 320–323.
[4] J.C. Ruiz-Morales, J. Canales-Vazquez, C. Savaniu, D. Marrero-Lopez, W.Z. Zhou, J.T.S. Irvine, Nature 439 (2006) 568–571.
[5] S. Tao, J.T.S. Irvine, J.A. Kilner, Adv. Mater. 17 (2005) 1734–1737.
[6] T. Ishihara, Bull. Chem. Soc. Jpn. 79 (2006) 1155–1166.
[7] Y.Z. Jiang, X.X. Xu, R. Lan, L. Zhang, S.W. Tao, J. Alloys Compd. 480 (2009) 874–877.
[8] X.X. Xu, S.W. Tao, J.T.S. Irvine, Solid State Ionics 180 (2009) 343–350.
[9] S. Wang, T. Kato, S. Nagata, T. Kaneko, N. Iwashita, T. Honda, M. Dokiya, Solid State Ionics 477 (2002) 152–153.
[10] B.C.H. Steele, Solid State Ionics 134 (2000) 3–20.
[11] B.C.H. Steele, Solid State Ionics 129 (2000) 95–110.
[12] T.S. Zhang, J. Ma, L.B. Kong, P. Hing, J.A. Kilner, Solid State Ionics 167 (2004) 191–196.
[13] Y.J. Leng, S.H. Chan, S.P. Jiang, K.A. Khor, Solid State Ionics 170 (2004) 9–15.
[14] C. Hatchwell, N.M. Sammes, I.W.M. Brown, Solid State Ionics 126 (1999) 201–208.
[15] J.A. Kilner, Chem. Lett. 37 (2008) 1012–1015.
[16] X.F. Guan, H.P. Zhou, Z.H. Liu, Y.A. Wang, J. Zhang, Mater. Res. Bull. 43 (2008) 1046–1054.
[17] B. Zhu, J. Power Sources 114 (2003) 1–9.
[18] B. Zhu, X.R. Liu, P. Zhou, Electrochem. Commun. 3 (2001) 566–571.
[19] J.B. Huang, Z.Q. Mao, Z.X. Liu, J. Power Sources 175 (2008) 238–243.
[20] J.Y. Cho, S.H. Hyun, S.A. Hong, J. Am. Ceram. Soc. 84 (2001) 937–940.
[21] J. Huang, Z. Mao, L. Yang, R. Peng, Electrochem. Solid-State Lett. 8 (2005) A437.
[22] R.D. Shannon, Acta Crystallogr. A32 (1976) 751.
[23] T.S. Zhanga, J. Maa, Y.J. Lengb, S.H. Chanb, P. Hinga, J.A. Kilner, Solid State Ionics 168 (2004) 187–195.
[24] C. Xia, Y. Li, Y. Tian, Q.H. Liu, Y.C. Zhao, L.J. Jia, Y.D. Li, J. Power Sources 188 (2009) 156–162.
[25] W. Zhu, C.R. Xia, D. Ding, X.Y. Shi, G.Y. Meng, Mater. Res. Bull. 41 (2006) 2057–2064.
[26] D.A. Keen, J. Phys.: Condens. Mat. 14 (2002) R189.
[27] S.P.S. Badwal, F.T. Ciacchi, J. Drennan, Solid State Ionics 121 (1999) 253–262.
[28] M. Mogensen, N.M. Sammes, G.A. Tompsett, Solid State Ionics 129 (2000) 63–94.
[29] H. Inaba, H. Tagawa, Solid State Ionics 83 (1996) 1–16.
[30] X.G. Zhang, M. Robertson, W. Qu, O. Kesler, R. Maric, D. Ghosh, J. Power Sources 164 (2007) 668–677.
[31] R.Q. Liu, Y.H. Xie, J.D. Wang, Z.J. Li, B.H. Wang, Solid State Ionics 17 (2006) 73–76.
[32] E. Ruiz-Trejo, J.A. Kilner, J. Appl. Electrochem. 39 (2009) 523–528.